Supplementary Information

Supplementary Information Figure S1. Immunoblot of GATE-16 in MEFs. The MEFs of the indicated genotype were cultured in the presence or absence of lysosomal inhibitors (E64d and pepstatin A: E/P) for 24 h. The cell lysates were subjected to SDS-PAGE and analyzed by immunoblotting with anti-GATE-16, anti-Atg3, and anti-actin antibodies. Data shown are representative of three separate experiments. While treatment of the inhibitors in wild-type MEFs led to appearance of GATE-16-II (PE-conjugated form), we recognized only GATE-16-I (free form) under both conditions in *Atg3*$^{-/-}$ MEFs. These results indicate that GATE-16-I was converted to GATE-16-II in wild-type but not *Atg3*-deficient MEFs, and GATE-16-II was degraded in lysosomes.

Supplementary Information Figure S2. Long exposure of images of the immunoblot data shown in Fig. 3A. Note that the amount of free Atg5 in *Atg3*-deficient MEFs increased significantly. Data represent three independent experiments.

Supplementary Information Figure S3. Appearance of dots positive for GFPAtg5 and Atg16L in *Atg3*-deficient MEFs is dependent on phosphatidylinositol 3-kinases. (**A**) Each wild-type and *Atg3*-deficient MEFs were pre-treated with a phosphatidylinositol 3-kinases inhibitor, Wortmannin (100 nM) for 2 h, and then cultured under nutrient-rich (non-deprived) or nutrient-poor (deprived) conditions in the presence or absence of Wortmannin.

Subsequently, the cells were fixed and then immunostained with anti-Atg16L. Bars; 10 μm. (**B**) The number of Atg16L-positive dots in MEF (n=20) was determined in each genotype. Data are mean±SD. $^{**}P<0.01$ by Student's *t*-test.

Supplementary Information Figure S4. Induction of autophagosome-like structures in *Atg3*-deficient MEFs was suppressed by treatment of phosphatidylinositol 3-kinases inhibitor, wortmannin. Each wild-type and *Atg3*-deficient MEFs were pre-treated with wortmannin (100 nM) for 2 h, and then cultured under nutrient-rich (non-deprived) or nutrient-poor (deprived) conditions in the presence or absence of wortmannin. They were fixed and processed for electron microscopy. The number of autophagosomes-like structures in each genotype was determined (n=20, for details, see Material and Methods). Data are mean±SD. $^{*}P<0.01$, by Student's *t*-test.

Supplementary Information Figure S5. Histology of major organs of $Atg3^{-/-}$ mice. Hematoxylin & eosin staining of sections from the major organs of $Atg3^{+/-}$ (left panels) and $Atg3^{-/-}$ (right panels) at 1 day after birth. Brain (**A** and **B**), thymus (**C** and **D**), heart (**E** and **F**), lung (**G** and **H**), liver (**I** and **J**), kidney (**K** and **L**), and intestine (**M** and **N**). Bars: 100 μm.

Supplementary Information Figure S6. *In vitro* reconstitution assay for Atg12-Atg5 conjugate formation. 0.1 μM of each protein (hAtg7, hAtg10, hAtg5 and hAtg12) and 5 mM ATP were reacted in the presence or absence of

hAtg3. The Atg12-Atg5 conjugates were detected by anti-Atg12 and anti-Atg5 antibodies. Note that Atg3 did not enhance the formation of Atg12-Atg5 conjugates *in vitro*. Representative data of similar results from three experiments.

Supplementary Information Videos 1 and 2. Time-lapse video microscopic analysis of the life span of GFPAtg5 dots in *Atg3*$^{+/+}$;GFPAtg5 (video 1) and *Atg3*$^{-/-}$;GFPAtg5 (video 2) MEFs. See Figure 4 for quantitative analysis. Bar: 2 μm.

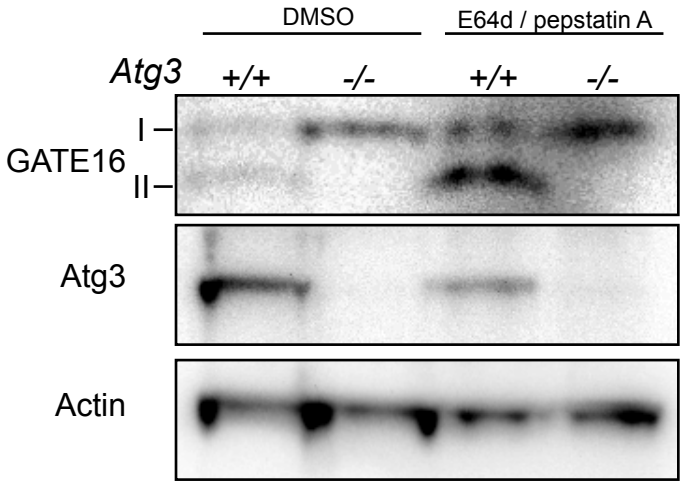

Y-s. Sou et al., Supplementary information figure S1

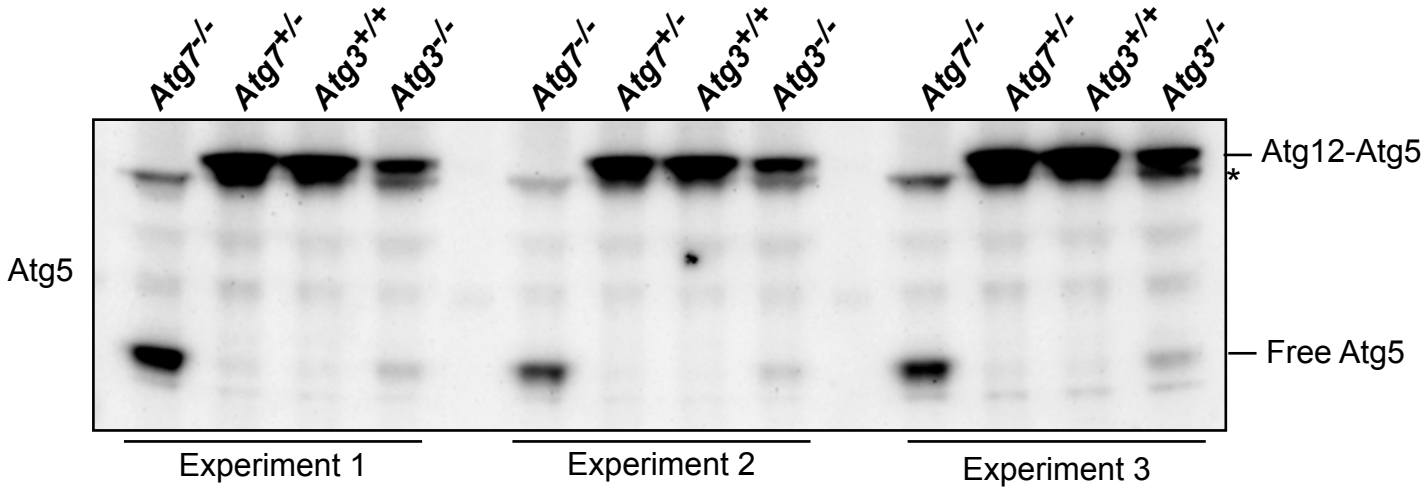

Y-s. Sou et al., Supplementary information figure S2

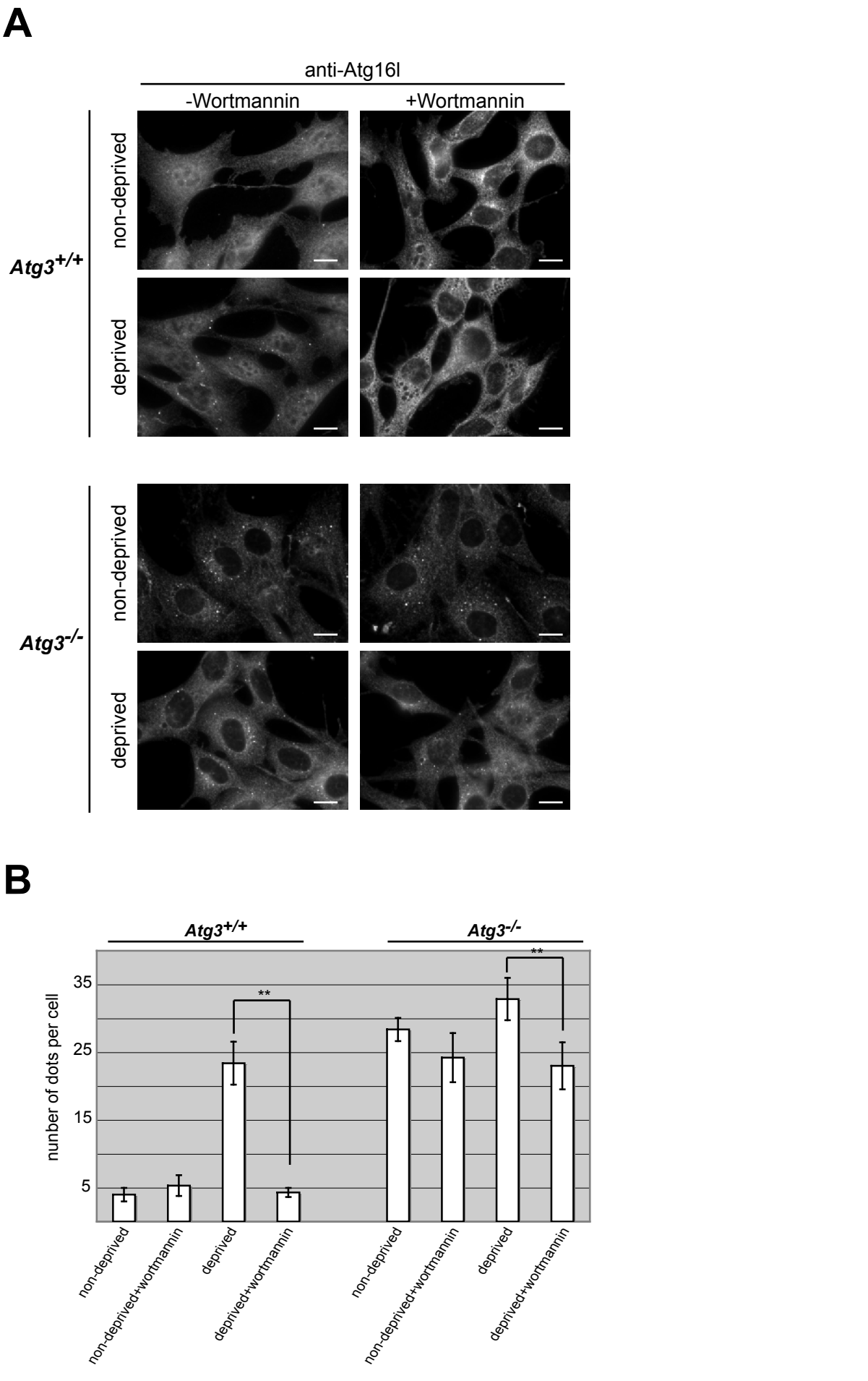

Y-s. Sou et al., Supplementary information figure S3

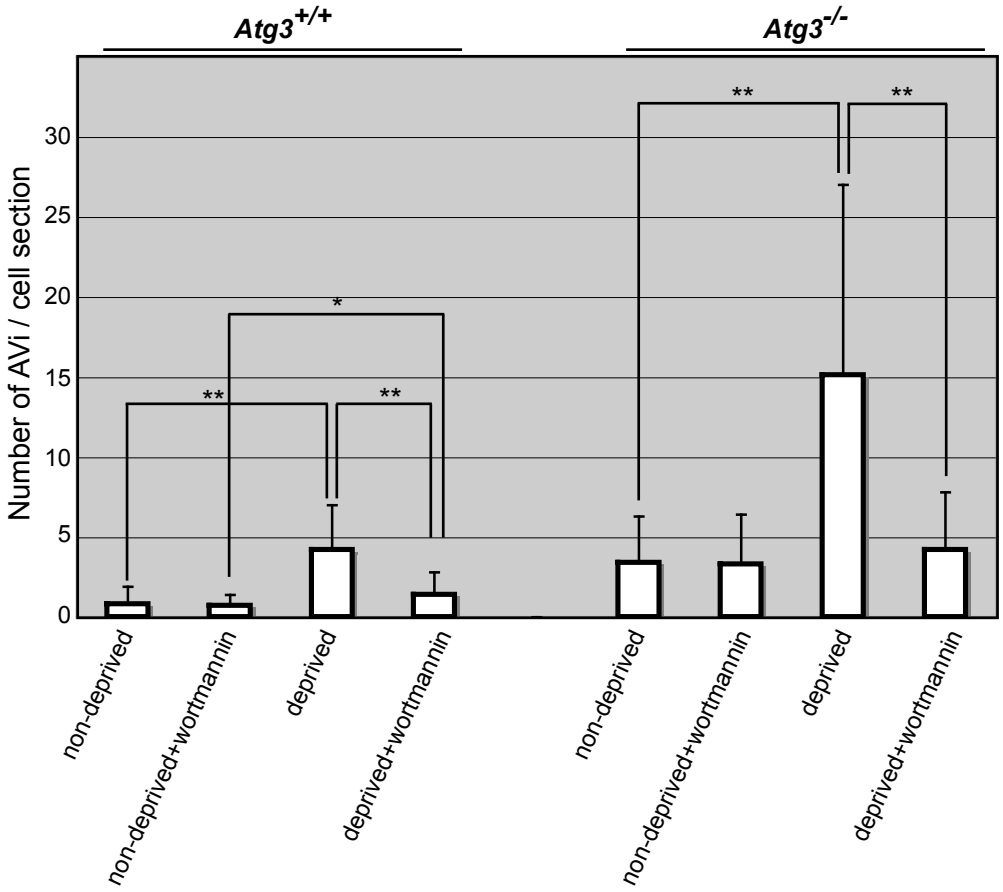

Y-s. Sou et al., Supplementary information figure S4

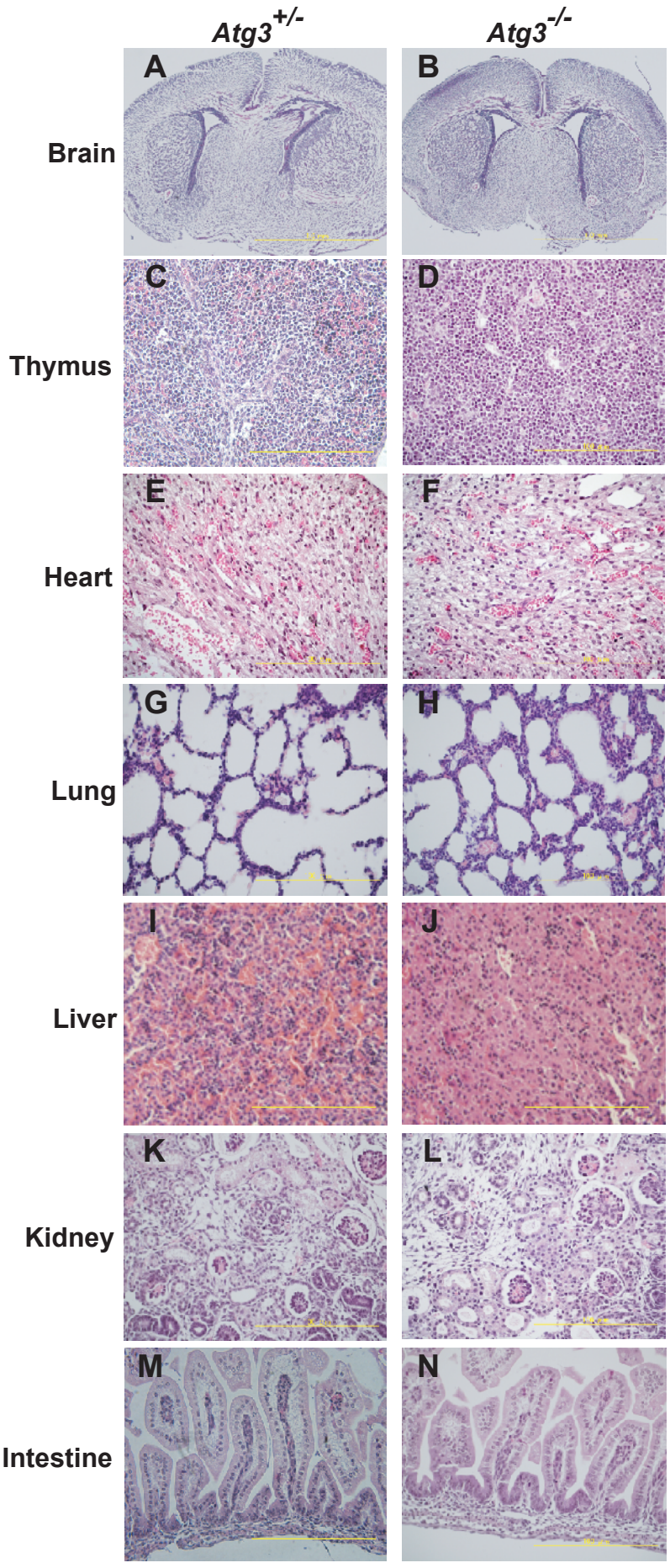

Y-s. Sou et al., Supplementary information figure S5

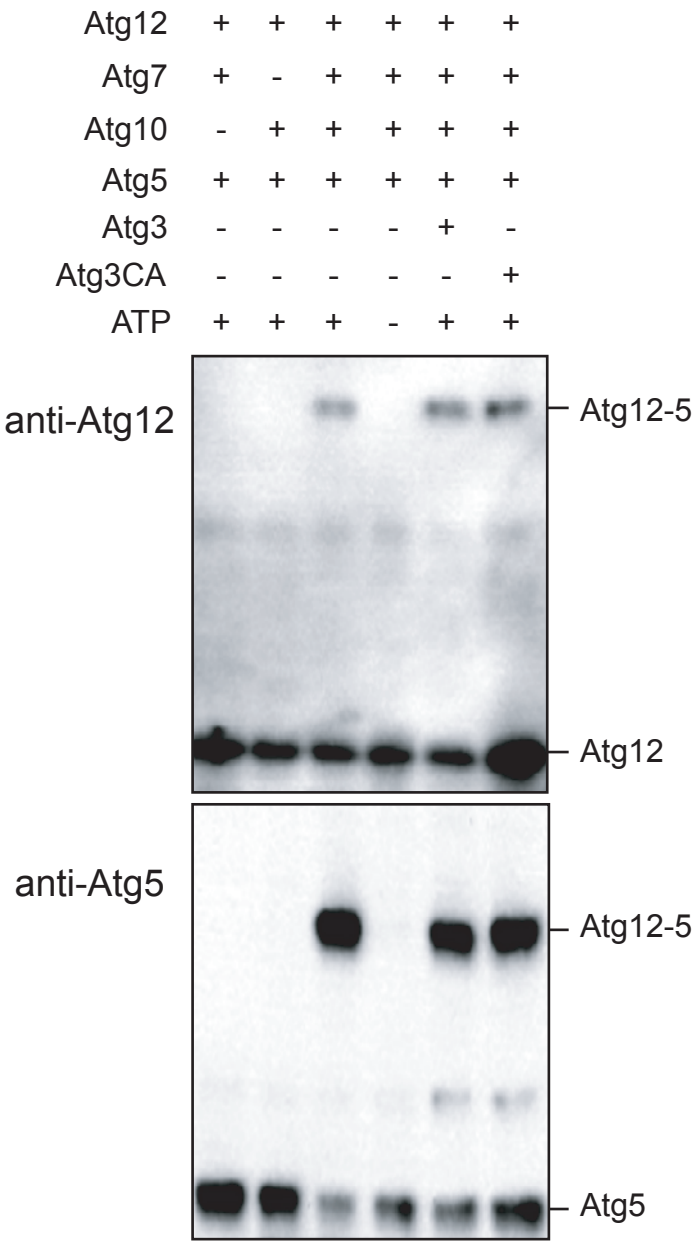

Y-s. Sou et al., Supplementary information figure S6